2021 American Control Conference (ACC)
New Orleans, USA, May 25-28, 2021

Stability and Control of Biomolecular Circuits through Structure

Fangzhou Xiao[1], Mustafa Khammash[2] and John C. Doyle[3]

Abstract— **Due to omnipresent uncertainties and environmental disturbances, natural and engineered biological organisms face the challenging control problem of achieving robust performance using unreliable parts. The key to overcoming this challenge rests in identifying structures of biomolecular circuits that are largely invariant despite uncertainties, and building control through such structures. In this work, we show that log derivatives can capture the structural regimes of biocircuits in regulating the production and degradation rates of molecules. We show that log derivatives can establish stability of fixed points based on structure, despite large variations in rates and functional forms of models. Furthermore, we demonstrate how control objectives, such as robust perfect adaptation (i.e. step disturbance rejection), could be implemented through structure. Due to the method's simplicity, structural properties for analysis and design of biomolecular circuits can often be determined by a glance at the equations.**

I. Introduction

Both natural and engineered cells face the challenge of achieving robust performance using unreliable parts [1]–[3]. In particular, the regulatory biomolecular circuits used in a cell are intrinsically stochastic and face large parameter uncertainties due to environmental disturbances as well as unknown or unintended interactions with host cell circuits.

Although feedback control has been successfully applied in electrical and mechanical engineering to achieve robust performance [4], it faces the new challenge in biological engineering that the parts are highly unreliable. Therefore it is essential to identify key structures of the uncertain behaviors in biomolecular circuits, so that control can be built on top of them.

Previous studies have identified several important structures of biomolecular circuits. While reaction rates tend to vary due to environmental disturbances, the stoichiometry of reactions are largely invariant. Indeed, stoichiometry could be robustly identified from experimental data and is often considered as structural information of a chemical reaction network [5], [6]. In addition, although rate constants and reactant concentrations vary due to disturbances, they often can be reliably determined or controlled up to orders-of-magnitude [7]. Lastly, the many reactions that happen in a cell often happen at different time scales, making descriptions of a circuit's behavior amenable to time-scale separation [8]. The most robust separation of time scales is the one between binding reactions and catalysis reactions, as exemplified by the Michaelis-Menten approximation, which has served as the foundation of dynamic modeling of biochemical reactions for over 100 years [9]–[11]. A simple physical argument is that binding reactions are fast as they mostly involve low-energy interactions such as hydrogen bonds, while catalysis modifies high-energy covalent bonds, therefore slower.

The structures mentioned above need to be synergistically integrated in a cohesive mathematical framework in order to analyze or design robustly performing biomolecular circuits using unreliable parts. In particular, it needs to connect structures with dynamical properties of the system. This difficult challenge, yet to be overcome, is the central cause for a major gap between the mathematical languages theorists use, and the mental pictures and diagrams that experimentalists use to guide their circuit designs and implementations [12]–[14].

This work provides initial results that could serve as a first attempt at filling this gap. In particular, we aim at building mathematical concepts that are tailored for these quintessentially biological structures.

In the following, we define a general class of systems, named birth-death systems, that emphasize the production and degradation of biomolecules, in Section II-A. In Section II-B, we use log derivatives to capture the structural regimes in production and degradation rates' dependence on reactant concentrations. In Section III, we show how log derivatives relate to a strong notion of stability of fixed points. Lastly, in Section IV, we show how control could be built on top of structures to achieve control goals such as robust perfect adaptation, biologists' term for step disturbance rejection.

A companion work with a focus on studies of examples that cater to a more biological audience is [15].

II. Structure in Biomolecular Systems

We begin by introducing the definition of birth death systems. We do so through chemical reaction networks (CRNs) [16] with biological growth.

A. Chemical Reaction Networks and Birth Death Systems

A CRN is a collection of reactions of the form

$$\alpha_{1j}X_1 + \cdots + \alpha_{nj}X_n \xrightarrow{k_j} \beta_{1j}X_1 + \cdots + \beta_{nj}X_n$$

where X_i, $i = 1, \ldots, n$ denote chemical species, $j = 1, \ldots, m$ index reactions, $\alpha_{ij}, \beta_{ij} \in \mathbb{Z}_{\geq 0}$ denote the number of X_i molecules consumed as reactant or produced as product in reaction j, and $k_j \in \mathbb{R}_{>0}$ is reaction rate constant of reaction j. We denote $\boldsymbol{\alpha}_j = \begin{bmatrix}\alpha_{1j} & \cdots & \alpha_{nj}\end{bmatrix}^\intercal$ as the reactant vector for reaction j, and similarly define $\boldsymbol{\beta}_j$ for

[1]Fangzhou Xiao is with Department of Biology and Biological Engineering, California Institute of Technology, 1200 E California Blvd., Pasadena, CA 91125, USA. xfz@caltech.edu

[2]Mustafa Khammash is with Department of Biosystems Science and Engineering, ETH Zurich, Mattenstrasse 26 4058 Basel, Switzerland., mustafa.khammash@bsse.ethz.ch

[3]John C. Doyle is with Department of Control and Dynamical Systems, California Institute of Technology, 1200 E California Blvd., Pasadena, CA 91125, USA., doyle@caltech.edu

978-1-6654-4197-1/$31.00 ©2021 AACC

product vector. We define $\boldsymbol{\gamma}_j = \boldsymbol{\beta}_j - \boldsymbol{\alpha}_j$ as the stoichiometry vector of reaction j, and collect them as columns to form the stoichiometry matrix $\boldsymbol{\Gamma} = \begin{bmatrix}\boldsymbol{\gamma}_1 & \cdots \boldsymbol{\gamma}_m\end{bmatrix} \in \mathbb{Z}^{n\times m}$.

The deterministic rate equation of the CRN is

$$\dot{\boldsymbol{x}} = \boldsymbol{\Gamma}\Lambda_{\boldsymbol{k}}\boldsymbol{\psi}(\boldsymbol{x}), \tag{1}$$

where $x_i \in \mathbb{R}_{\geq 0}$ is the concentration of species X_i, $\Lambda_{\boldsymbol{k}} := \operatorname{diag}\{\boldsymbol{k}\}$ is a diagonal matrix with reaction rate constants k_j as entries, and $\psi(\boldsymbol{x}) : \mathbb{R}^n_{\geq 0} \to \mathbb{R}^m_{\geq 0}$ denote how the rate of reactions depend on concentrations.

A commonly used specification for $\psi_j(\boldsymbol{x})$ is the law of mass-action, which is applicable to a wide range of scenarios [17]. It says $\psi_j(\boldsymbol{x}) = \boldsymbol{x}^{\boldsymbol{\alpha}_j}$, where we denote $\boldsymbol{x}^{\boldsymbol{\alpha}_j} = \prod_{i=1}^n x_i^{\alpha_{ij}}$.

Since concentrations of biomolecules change by production and degradation reactions, we could re-write the dynamics as follows:

$$\dot{x_i} = f_i(\boldsymbol{x}) =: f_i^+(\boldsymbol{x}) - f_i^-(\boldsymbol{x}) \tag{2}$$

$$:= \sum_{j:\gamma_{ij}>0} k_j\gamma_{ij}\psi_j(\boldsymbol{x}) - \sum_{j:\gamma_{ij}<0} k_j\gamma_{ij}\psi_j(\boldsymbol{x}) \tag{3}$$

where we have collected terms from reactions producing x_i into $f_i^+(\boldsymbol{x})$ and terms from reactions degrading x_i into $f_i^-(\boldsymbol{x})$.

The physical interpretation of the variables x_i as concentrations dictate that they remain non-negative, therefore the positive orthant is forward invariant. A necessary and sufficient condition is $f_i(\boldsymbol{x}) \geq 0$ whenever $x_i = 0$. It is also natural to assume that each species has at least one production reaction and at least one degradation reaction. This yields the following definition for birth-death systems.

Definition 1: A birth-death system is a dynamical system of the form (2) where the production and degradation rates $f_i^\pm : \mathbb{R}^n_{\geq 0} \to \mathbb{R}_{\geq 0}$ are analytic and globally non-negative, and $f_i(\boldsymbol{x}) \geq 0$ whenever $x_i = 0$.

Note that although CRNs are used here to introduce the context, the definition of birth-death systems is independent of any underlying CRNs.

The definition of a birth-death system emphasizes the structure that the concentration of each species is regulated by two processes, production and degradation. Understanding the dynamics of a birth-death system then comes down to characterizing how production and degradation rates $f_i^\pm(\boldsymbol{x})$ depend on the concentrations $\boldsymbol{x}$. In the following section, we use a simple example to illustrate that the dependence of $f_i^\pm(\boldsymbol{x})$ on $\boldsymbol{x}$ is highly structured, and this structure could be formalized through log derivatives.

B. Log derivatives formalize structural regimes of regulation under time-scale separation

Production and degradation of molecules happen through enzymatic catalysis [10]. In the following, we consider the simplest regulation of enzymatic catalysis to illustrate the structure in $f_i^\pm(\boldsymbol{x})$'s dependence on $\boldsymbol{x}$.

$$E + S \underset{k_-}{\overset{k_+}{\rightleftharpoons}} C \xrightarrow{k_f} E + P. \tag{4}$$

Here E is the enzyme, S is substrate, C is the complex formed from E and S binding together, and P is the product molecule formed.

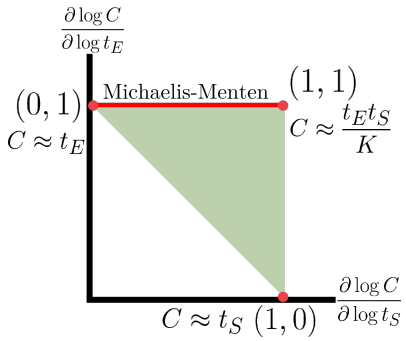

Fig. 1: The log-derivative polytope of the complex C with respect to t_E and t_S defined by steady state equations in Eq (5). A point in this space represents the sensitivity of the steady-state C concentration to changes in the total concentration of E or S. The green triangle marks the possible sensitivity values the system can admit. The edges of the triangle represent different assumptions about the saturation of the species. The edge marked by the red line is the range of log derivatives covered by the Michaelis-Menten formula. Red dots mark the vertices. The expressions next to the vertices correspond to the three regimes.

To proceed, we use time-scale separation that binding reactions tend to be much faster than catalysis reactions. This entails the following equations:

$$t_E = E + C, \quad t_S = C + S, \quad C = \frac{ES}{K}, \tag{5}$$

where we slightly abuse notation to use symbol of species X to also denote its concentration. Here t_E is the total concentration of enzyme E, t_S is total concentration of substrate S, and K is the dissociation constant K_d or its variants such as K_M, based on details of which part of C dynamics is considered fast [18].

To connect with the notation of birth-death systems, we denote x_P as the concentration of P, $x_E := t_E$ as the total concentration of E, and $x_S := t_S$ as the total concentration of S. Then x_P's dynamics is

$$\dot{x}_P = f_P^+ - f_P^- = k_f C(x_E, x_S) - 0, \tag{6}$$

where $C(x_E, x_S)$ is the steady state concentration of C in terms of total concentrations of E and S in Eq (5).

In order to understand how f_P^+, the production rate of x_P, depends on x_E and x_S, we need to solve for C in terms of t_E and t_S in Eq (5). A classical way to approach this is the Michaelis-Menten approximation [18], which assumes the total concentration of the substrate is much higher than that of the enzyme, i.e. $t_S \gg t_E$. This implies $t_S \approx S$, therefore Eq (5) solves to be

$$C(t_E, t_S) \approx t_E \frac{t_S}{t_S + K}. \tag{7}$$

This expression could be intuitively understood as containing two regimes. One has $t_S \gg K$, so that $C \approx t_E$. This is constant in t_S, therefore "substrate-saturated". The other one has $t_S \ll K$, so that $C \approx \frac{t_E t_S}{K}$. This is linear in t_S, therefore "substrate-sensitive". We note that these two regimes have distinct exponents in t_E and t_S: $(1,0)$ for the saturated regime, and $(1,1)$ for the sensitive regime (see Figure 1).

Therefore, although f_P^+, the production rate of x_P, depends on concentrations and rates that tend to vary, the fact

that there are two regimes with distinct exponents $(1,0)$ and $(1,1)$ is structurally determined. Indeed, the exponents fundamentally come from the stoichiometry of the binding reaction in Eq (4). In addition, the condition such that one regime is valid, such as $t_S \gg t_E, K$, only depend on the orders of magnitude of the concentrations and rates, therefore could be reliably determined or controlled.

Now, we would like to describe these regimes and their exponents in a formal way. For this purpose, we introduce log derivatives as differential analogues of exponents. For example, from Eq (7) we calculate

$$\begin{bmatrix} \frac{\partial \log C}{\partial \log t_E} & \frac{\partial \log C}{\partial \log t_S} \end{bmatrix} = \begin{bmatrix} 1 & \frac{K}{t_S+K} \end{bmatrix}. \tag{8}$$

When $t_S \gg K$, we obtain log derivative $(1,0)$; while when $t_S \ll K$, we obtain $(1,1)$. So log derivatives exactly capture the exponents of the regimes in a continuous way.

With the tool of log derivatives in mind, we could actually go back and obtain more general results than the Michaelis-Menten approximation. Indeed, due to the assumption that $t_S \gg t_E$, we missed the third "enzyme-saturated" regime: when $t_E \gg t_S, K$, we have $C \approx t_S$. Capturing this regime is important if the $t_S \gg t_E$ assumption does not hold all the time, such as when S and E are molecules of similar abundance in protein binding, or when the cellular circuit has highly dynamic behavior during nutrient shifts or shock responses [19], [20].

To capture all three regimes, we need to do away with assumptions like Michaelis-Menten. Although the steady state equations in Eq (5) can be directly solved in this simple case, this procedure results in a cumbersome expression that fails to generalize. More importantly, the explicit expression hides the structures in the exponents of the regimes mentioned above. In contrast, the differential description through log derivatives can capture all three regimes while describing the exponents. Indeed, applying implicit function theorem to Eq (5) to solve for the expression of E, S, C in terms of t_E, t_S, K yields the following result:

$$\begin{bmatrix} \frac{\partial \log C}{\partial \log t_E} & \frac{\partial \log C}{\partial \log t_S} \end{bmatrix} = \begin{bmatrix} \frac{K+E}{K+E+S} & \frac{K+S}{K+E+S} \end{bmatrix}. \tag{9}$$

This shows that the log derivatives of C with respect to t_E and t_S take values inside a triangle (see Figure 1), and the exact location in the triangle depends on the particular values of t_E, t_S and K. Completely in accordance with our intuition, the vertices of this triangle correspond to the three regimes described earlier. In particular, we see that the Michaelis-Menten approximation is just one edge of this triangle, a strict subset of the behaviors captured by the log derivatives.

The fact that the log derivatives form a triangle, i.e. the set of convex combinations of the three vertices, suggests that the full behavior of this enzymatic catalysis could be seen as combinations of the three regimes corresponding to the three vertices. Indeed, when the corresponding asymptotic conditions are satisfied, the behavior of the enzyme regulation is essentially the same as the simple monomials at the vertices. Extending this to all production and degradation fluxes, we see that a general birth-death system could be seen as having several regimes, each corresponding to a simple system with constant exponents. Depending on the location of the state, the system could be approximated by one or another simple system corresponding to the closest regime. Hence the following definition.

Definition 2: A *simple birth-death system* is a birth-death system with $f_i^{\pm}(\boldsymbol{x}) = k_i^{\pm}\boldsymbol{x}^{\boldsymbol{\alpha}_i^{\pm}}$, where $\boldsymbol{\alpha}_i^{\pm} \in \mathbb{R}^n$ is a constant vector, and $k_i^{\pm} > 0$ is a positive constant.

Simple birth-death systems have the advantage that their log derivatives can be directly read off from the exponent vector in the rate functions. In contrast, obtaining the set of log derivatives that emerges directly from binding networks is nontrivial in general. Next, we show that log derivatives do form easily-identified polytopes in most models of biological circuits, where polynomials and Hill functions from Michaelis-Menten approximations are used.

C. Basic facts about log derivatives

Here are some basic calculations to facilitate intuition about log derivatives.

If f_i^+ is a monomial, i.e. $f_i^+(\boldsymbol{x}) = k_j^+\boldsymbol{x}^{\boldsymbol{\alpha}_j^+}$, then $H_{i\ell}^+ = \alpha_{j\ell}^+$ for $\ell = 1, \ldots, n$. In other words, the log derivative vector $\boldsymbol{H}_i^+$ for the production of X_i is the exponent vector $\boldsymbol{\alpha}_j^+$, independent of the rate constant k_j^+ or concentration $\boldsymbol{x}$. This case corresponds to simple birth death system. Physically, this case could happen when X_i has only one production reaction. Then $\boldsymbol{\alpha}_j^+$ is the reactant stoichiometry vector for that production reaction.

If $f_i^+ \in \mathbb{R}_{>0}[\boldsymbol{x}]$ is a multivariate polynomial in $\boldsymbol{x}$ with positive coefficients, i.e. $f_i^+(\boldsymbol{x}) = \sum_{j\in J_i} k_j\boldsymbol{x}^{\boldsymbol{\alpha}_j}$ for index set $J_i^+ = \{j : \gamma_{ji} > 0\}$ of all reactions producing X_i, then

$$H_{i\ell}^+(\boldsymbol{x}) = \sum_{j\in J_i^+} \lambda_j(\boldsymbol{x})\alpha_{j\ell}, \quad \lambda_j(\boldsymbol{x}) = \frac{k_j\boldsymbol{x}^{\boldsymbol{\alpha}_j}}{\sum_{j\in J_i^+} k_j\boldsymbol{x}^{\boldsymbol{\alpha}_j}}. \tag{10}$$

Since $\lambda_j > 0$ and sums to one, the log derivative vector for the production rate of X_i is the convex combination of the reactant vectors of all X_i-producing reactions. In other words, $\boldsymbol{H}_i^+(\boldsymbol{x}) \in P(f_i^+) := \operatorname{conv}\{\boldsymbol{\alpha}_j : j \in J_i^+\}$, where $P(f_i^+)$ is the Newton polytope of polynomial f_i^+. Although the location in the polytope depends on k_j and $\boldsymbol{x}$, the polytope itself depends on reactant vectors $\boldsymbol{\alpha}_j$ alone. We note that newton polytopes are fruitful tools in analysis and optimization of polynomial equations, dynamical systems, and CRNs [21]–[23].

If f_i^+ is a rational function with the numerator as one term of the denominator polynomial, i.e.

$$f_i^+(\boldsymbol{x}) = \frac{k_{j'}\boldsymbol{x}^{\alpha_{j'}}}{\sum_{j\in J_i^+} k_j\boldsymbol{x}^{\boldsymbol{\alpha}_j}}, \tag{11}$$

which typically arises from time-scale separations and Michaelis-Menten type approximations, then

$$H_{i\ell}^+(\boldsymbol{x}) = \sum_{j\neq j'} \lambda_j(\boldsymbol{x})(\alpha_{j'\ell} - \alpha_{j\ell}), \tag{12}$$

where λ_j is the same as before. In this case, the log derivative vector for production of X_i is the convex combination of all reactions' reactant vectors minus the numerator reactant vector: $\boldsymbol{H}_i^+(\boldsymbol{x}) \in \operatorname{conv}\{\boldsymbol{\alpha}_{j'} - \boldsymbol{\alpha}_j : j \in J_i^+\} = \boldsymbol{\alpha}_{j'} - P(f_i^+)$.

The above calculations enable writing down log derivatives immediately after a glance at the equation in many cases, making log derivatives easy to use.

D. Dilution due to Biological Growth

Many biomolecular circuits in systems and synthetic biology do not contain degradation reactions. Instead, the production of molecules are balanced by dilution due to increase in reaction volume from cell growth. For completeness, here we briefly show that dilution can be captured in birth-death systems for a homogeneous population of cells, but it has distinct structures.

For a homogeneous population of cells where each cell has the same volume and number of molecules, denote each cell's volume by v_0, and the number of cells by N. Let $X_i^{\text{tot}} = x_i v_0 N$ denote the total number of X_i molecules in this population, then

$$\dot{x}_i = \frac{d}{dt}\frac{X_i^{\text{tot}}}{N v_0} = \frac{1}{N v_0}\dot{X}_i^{\text{tot}} - \frac{X_i^{\text{tot}}}{v_0 N^2}\dot{N}. \tag{13}$$

Let $f_i^{\pm}$ denote the production and degradation rates for species i in every cell due to chemical reactions. So the rate of change for the total count of X_i is $\dot{X}_i^{\text{tot}} = f_i(\boldsymbol{x}) v_0 N$. Let $f^{\text{g}}(\boldsymbol{x})$ denote the growth rate of the population, assumed independent of N and v_0, then $\dot{N} = f^g(\boldsymbol{x})N$. Hence,

$$\dot{x}_i = f_i^+(\boldsymbol{x}) - f_i^-(\boldsymbol{x}) - f^g(\boldsymbol{x}) x_i. \tag{14}$$

We see that this is still a birth-death system, with dilution considered as a term in degradation. However, dilution has the unique structure that it adds the same term times x_i for each species i.

III. Structure and Fixed Point Stability

We have shown that the structures of biomolecular circuits could be captured via log derivatives. In the following, we discuss how log derivatives connect with fixed point stability in birth-death systems. We show that log derivatives could certify structural stability of a fixed point: stability that is independent of concentrations and rates.

A. Linearization and logarithmic derivatives

We first assume that the birth-death system has a positive fixed point $\boldsymbol{x}^* \in \mathbb{R}^n_{>0}$ such that $\boldsymbol{f}(\boldsymbol{x}^*) = 0$, with positive production and degradation fluxes: $\boldsymbol{f}^{\pm}(\boldsymbol{x}^*) \in \mathbb{R}^n_{>0}$.

To express the linearization of a birth-death system in terms of log derivatives, we introduce the log derivative map

$$\boldsymbol{H}(\boldsymbol{f}^{\pm}, \boldsymbol{x}) := \frac{\partial \log \boldsymbol{f}^{\pm}}{\partial \log \boldsymbol{x}}(\boldsymbol{x}), \tag{15}$$

where $\log$ is applied component-wise. The log derivative map takes a positive function $\boldsymbol{f}^{\pm}$ and a point $\boldsymbol{x}$ in its domain to the function's log derivative at this point. For simplicity, we denote $\boldsymbol{H}^{\pm} := \boldsymbol{H}(\boldsymbol{f}^{\pm}, \boldsymbol{x})$, and $\boldsymbol{H} := \boldsymbol{H}^+ - \boldsymbol{H}^-$.

Derivatives in terms of log derivatives is

$$\frac{\partial f_i^{\pm}(\boldsymbol{x})}{\partial x_j} = \frac{\partial \log f_i^{\pm}(\boldsymbol{x})}{\partial \log x_j}\frac{f_i^{\pm}(\boldsymbol{x})}{x_j} = H_{ij}^{\pm}\frac{f_i^{\pm}(\boldsymbol{x})}{x_i}\frac{x_i}{x_j}. \tag{16}$$

In matrix form, this is

$$\frac{\partial \boldsymbol{f}(\boldsymbol{x})}{\partial \boldsymbol{x}} = \boldsymbol{\Lambda}_{\boldsymbol{x}}\left(\boldsymbol{\Lambda}_{\boldsymbol{\tau}^+}^{-1}\boldsymbol{H}^+ - \boldsymbol{\Lambda}_{\boldsymbol{\tau}^-}^{-1}\boldsymbol{H}^-\right)\boldsymbol{\Lambda}_{\boldsymbol{x}}^{-1}, \tag{17}$$

where $\tau_i^{\pm}(\boldsymbol{x}) := \frac{x_i}{f_i^{\pm}(\boldsymbol{x})}$ are time-scales of X_i's production and degradation [24], [25].

At a fixed point $\boldsymbol{x}^*$, we have $\boldsymbol{f}^+(\boldsymbol{x}^*) = \boldsymbol{f}^-(\boldsymbol{x}^*)$, so we could define $\boldsymbol{\tau} := \boldsymbol{\tau}^+(\boldsymbol{x}^*) = \boldsymbol{\tau}^-(\boldsymbol{x}^*)$ as the vector of steady-state time-scales at fixed point $\boldsymbol{x}^*$. Therefore, we have

$$\boldsymbol{A} := \frac{\partial \boldsymbol{f}}{\partial \boldsymbol{x}}(\boldsymbol{x}^*) = \boldsymbol{\Lambda}_{\boldsymbol{x}^*}\boldsymbol{\Lambda}_{\boldsymbol{\tau}}^{-1}\boldsymbol{H}\boldsymbol{\Lambda}_{\boldsymbol{x}^*}^{-1}, \tag{18}$$

relating linearized dynamics $\boldsymbol{A}$ to log derivative matrix $\boldsymbol{H}$.

Define $\boldsymbol{M} := \boldsymbol{\Lambda}_{\boldsymbol{\tau}}^{-1}\boldsymbol{H}$. Since $\boldsymbol{A}$ and $\boldsymbol{M}$ are similar to each other, they have the same eigenvalues. So we immediately see that the fixed point $\boldsymbol{x}^*$ is stable if and only if $\boldsymbol{M}$ is Hurwitz. Therefore, the stability of the fixed point $\boldsymbol{x}^*$ depends only on $\boldsymbol{M}$, which nicely splits into two parts: the time-scales in $\boldsymbol{\Lambda}_{\boldsymbol{\tau}}^{-1}$, and the log derivatives in $\boldsymbol{H}$. Since the time-scales come from uncertain rates and concentrations, while log derivatives capture reliable structural regimes of the system, this prompts the following definition.

Definition 3: A fixed point $\boldsymbol{x}^*$ of a birth-death system is *structurally stable* if it is stable for all positive analytic rate functions $\boldsymbol{f}^{\pm}$ that leave the log derivative matrix $\boldsymbol{H}$ at $\boldsymbol{x}^*$ invariant.

In terms of $\boldsymbol{M}$, since $\boldsymbol{H}$ is assumed constant while $\boldsymbol{\tau}$ can vary, the definition of structural stability exactly corresponds to that the $\boldsymbol{H}$ is (multiplicative) D-stable in matrix analysis. In other words, left multiplication of $\boldsymbol{H}$ by arbitrary positive diagonal matrices results in a Hurwitz matrix (see extensive review by [26]). D-stability has been extensively studied since the very beginning of control theory, yet a clean necessary and sufficient characterization has not been found. This is in part due to the topological pathology of this property, that the set of D-stable matrices is neither closed nor open. One sufficient condition of D-stability that characterizes a topologically nice (open) set of matrices is diagonal stability.

Definition 4: A matrix $\boldsymbol{H}$ is *diagonally stable* if there exists a positive diagonal matrix $\boldsymbol{P}$ such that

$$\boldsymbol{P}\boldsymbol{H} + \boldsymbol{H}^{\intercal}\boldsymbol{P} < 0, \tag{19}$$

where < 0 for matrices denote negative definiteness.

Since Eq (19) is a linear matrix inequality, scalable numerical solution algorithms are available off-the-shelf.

A theorem summarizes above discussions.

Theorem 5: $\boldsymbol{H}$ is diagonally stable implies the fixed point $\boldsymbol{x}^*$ is structurally stable. $\boldsymbol{H}$ is diagonally stable if and only if $\boldsymbol{A}$ is diagonally stable.

Proof: We calculate that

$$\begin{aligned}\boldsymbol{P}\boldsymbol{H} + \boldsymbol{H}^{\intercal}\boldsymbol{P} &= \boldsymbol{P}\boldsymbol{\Lambda}_{\boldsymbol{\tau}}\boldsymbol{\Lambda}_{\boldsymbol{\tau}}^{-1}\boldsymbol{H} + (\boldsymbol{\Lambda}_{\boldsymbol{\tau}}^{-1}\boldsymbol{H})^{\intercal}\boldsymbol{\Lambda}_{\boldsymbol{\tau}}\boldsymbol{P} \\ &= \tilde{\boldsymbol{P}}\boldsymbol{M} + \boldsymbol{M}^{\intercal}\tilde{\boldsymbol{P}},\end{aligned}$$

where $\tilde{\boldsymbol{P}} = \boldsymbol{\Lambda}_{\boldsymbol{\tau}}\boldsymbol{P}$. Therefore, $\boldsymbol{H}$ is diagonally stable is equivalent to $\boldsymbol{M}$ is diagonally stable, which is equivalent to $\boldsymbol{A}$ is diagonally stable as they are similar through positive diagonal matrix multiplications. ∎

There are a few special cases of the above theorem that is worth mentioning due to their simplicity.

Corollary 6: Any of the following conditions imply $\boldsymbol{x}^*$ is structurally stable.

1) $\boldsymbol{H}$ is triangular with negative diagonal entries.

2) $\boldsymbol{H}$ is symmetric and negative definite.
3) The symmetrization of $\boldsymbol{H}$, $\mathrm{Re}\boldsymbol{H} := \frac{1}{2}(\boldsymbol{H} + \boldsymbol{H}^\intercal)$, is negative definite.

Structural methods could be easily extended to certify fixed points' structural instability as well. This is because when $\boldsymbol{H}$ has no purely imaginary eigenvalues, any symmetric matrix $\boldsymbol{P}$ that satisfies Eq (19) has inertia (i.e. signs of eigenvalues' real parts) that are opposite to the inertia of $\boldsymbol{H}$, as stated in the Ostroski-Schneider theorem in matrix analysis [26], [27]. Therefore, if there exists a diagonal matrix $\boldsymbol{P}$ with at least one negative entry satisfying Eq (19), then $\boldsymbol{H}$ is not Hurwitz, and $\boldsymbol{\Lambda}_{\boldsymbol{\tau}}^{-1}\boldsymbol{H}$ is not Hurwitz for all positive vectors $\boldsymbol{\tau}$. We summarize this into the following theorem.

Theorem 7: Given a birth-death system as in (2) with log derivative matrix $\boldsymbol{H}$ at a positive fixed point $\boldsymbol{x}^*$, if $\boldsymbol{H}$ has no purely imaginary eigenvalues and there exists a diagonal matrix $\boldsymbol{P}$ with at least one negative entry such that Eq (19) holds, then $\boldsymbol{x}^*$ is structurally unstable, i.e. it is unstable for all positive analytic functions $\boldsymbol{f}^\pm$ that keeps $\boldsymbol{H}$ invariant.

IV. Control through Structure

We have shown that fixed point structural stability could be quickly determined from log derivatives. In the following, we show that robust perfect adaptation (RPA), biologists' term for step disturbance rejection, can be implemented through log derivatives.

A. Birth-death control systems

We start by extending closed birth-death dynamical systems to open birth-death control systems.

Definition 8: A *birth-death control system* is

$$\begin{aligned} \dot{\boldsymbol{x}} &= \boldsymbol{f}(\boldsymbol{x}, \boldsymbol{w}) = \boldsymbol{f}^+(\boldsymbol{x}, \boldsymbol{w}) - \boldsymbol{f}^-(\boldsymbol{x}, \boldsymbol{w}), \\ \boldsymbol{y} &= \boldsymbol{h}(\boldsymbol{x}, \boldsymbol{w}), \end{aligned} \tag{20}$$

where $\boldsymbol{x} \in \mathbb{R}^n_{\geq 0}$ is state, $\boldsymbol{w} \in \mathbb{R}^n_{\geq 0}$ is disturbance input, and $\boldsymbol{y} \in \mathbb{R}^p$ is output. The analytic functions $\boldsymbol{f}^\pm : \mathbb{R}^n_{\geq 0} \times \mathbb{R}^d_{\geq 0} \to \boldsymbol{R}^n_{\geq 0}$ are production and degradation rates, and $\boldsymbol{h} : \mathbb{R}^n_{\geq 0} \times \mathbb{R}^d_{\geq 0} \to \mathbb{R}^p_{\geq 0}$ is output function.

Note that to keep the biological plausibility that disturbances and outputs come from rates and concentrations, the variables $\boldsymbol{w}$ and $\boldsymbol{y}$ are also assumed to be non-negative.

In the following, we restrict our attention to the single-intput-single-output (SISO) case, so w and y are scalars.

B. Linearized dynamics in terms of log derivatives

We assume the birth-death control system admits a positive reference point $(\boldsymbol{x}^*, w^*) \in \mathbb{R}^n_{>0} \times \mathbb{R}_{>0}$ such that $\boldsymbol{f}(\boldsymbol{x}^*, w^*) = 0$ with positive outputs and rates: $\boldsymbol{f}^\pm(\boldsymbol{x}^*, w^*) > 0$, $y^* := h(\boldsymbol{x}^*, w^*) > 0$. Linearizing the system at this reference point then yields the following system.

$$\begin{aligned} \dot{\boldsymbol{\varepsilon}} &= \boldsymbol{A}\boldsymbol{\varepsilon} + \boldsymbol{b}\delta, \\ z &= \boldsymbol{c}\boldsymbol{\varepsilon} + d\delta, \end{aligned} \tag{21}$$

where $\varepsilon_i \approx x_i - x_i^*$, $\delta \approx w - w^*$, $z \approx y - y^*$ are linearized variables of x_i, w and y. The matrices are $\boldsymbol{A} = \partial_{\boldsymbol{x}} \boldsymbol{f}(\boldsymbol{x}^*, w^*) \in \mathbb{R}^{n\times n}$, $\boldsymbol{b} = \partial_w \boldsymbol{f}(\boldsymbol{x}^*, w^*) \in \mathbb{R}^{n\times 1}$, $\boldsymbol{c} = \partial_{\boldsymbol{x}} h(\boldsymbol{x}^*, w^*) \in \mathbb{R}^{n\times 1}$, and $d = \partial_w h(\boldsymbol{x}^*, w^*)$.

To express the linearized dynamics in log derivatives, we change variables into multiplicative deviations instead of additive difference:

$$\begin{aligned} \dot{\tilde{\boldsymbol{\varepsilon}}} &= \boldsymbol{\Lambda}_{\boldsymbol{\tau}}^{-1} \left(\boldsymbol{H}^A \tilde{\boldsymbol{\varepsilon}} + \boldsymbol{H}^b \tilde{\delta} \right), \\ \tilde{z} &= \boldsymbol{H}^c \tilde{\boldsymbol{\varepsilon}} + H^d \tilde{\delta}, \end{aligned} \tag{22}$$

where $\tilde{\varepsilon}_i = \frac{\varepsilon_i}{x_i^*}$, $\tilde{\delta} = \frac{\delta}{w^*}$, $\tilde{z} = \frac{z}{y^*}$ are fold-change linearized variables of x_i, w and y. The log derivative matrices are

$$\begin{bmatrix} \boldsymbol{H}^A & \boldsymbol{H}^b \\ \boldsymbol{H}^c & H^d \end{bmatrix} = \begin{bmatrix} \frac{\partial \log \boldsymbol{f}^+ - \log \boldsymbol{f}^-}{\partial \log \boldsymbol{x}} & \frac{\partial \log \boldsymbol{f}^+ - \log \boldsymbol{f}^-}{\partial \log w} \\ \frac{\partial \log h}{\partial \log \boldsymbol{x}} & \frac{\partial \log h}{\partial \log w} \end{bmatrix} \tag{23}$$

with the right hand side functions evaluated at $(\boldsymbol{x}^*, w^*)$. $\tau_i := \frac{x_i^*}{f_i^\pm(\boldsymbol{x}^*, w^*)}$ is the reference time-scale as before. The following relates the two versions of linearized dynamics:

$$\begin{bmatrix} \boldsymbol{A} & \boldsymbol{b} \\ \boldsymbol{c} & d \end{bmatrix} = \begin{bmatrix} \boldsymbol{\Lambda}_{\boldsymbol{\tau}}^{-1} \boldsymbol{\Lambda}_{\boldsymbol{x}} \boldsymbol{H}^A \boldsymbol{\Lambda}_{\boldsymbol{x}}^{-1} & \frac{1}{w^*} \boldsymbol{\Lambda}_{\boldsymbol{\tau}}^{-1} \boldsymbol{\Lambda}_{\boldsymbol{x}} \boldsymbol{H}^b \\ y^* \boldsymbol{H}^c \boldsymbol{\Lambda}_{\boldsymbol{x}}^{-1} & \frac{y^*}{w^*} H^d \end{bmatrix}. \tag{24}$$

From this, we see that the transfer function for the fold-change linearized system is

$$\tilde{G}(s) = H^d + \boldsymbol{H}^c \left(s\boldsymbol{\Lambda}_{\boldsymbol{\tau}} - \boldsymbol{H}^A \right)^{-1} \boldsymbol{H}^b. \tag{25}$$

In fact, the fold-change transfer function is proportional to the transfer function of the additive variables: $G(s) := d + \boldsymbol{c}(s\boldsymbol{I} - \boldsymbol{A})^{-1}\boldsymbol{b} = \frac{y^*}{w^*}\tilde{G}(s)$.

These calculations prepare us to discuss robust perfect adaptation based on structure.

C. Structural robust perfect adaptation

Maintaining homeostasis despite uncertainties and disturbances is an essential function for biological organisms. Because of this, biomolecular circuits that achieve robust perfect adaptation (RPA) have been actively studied in systems biology [28]–[31] and synthetic biology [32], [33]. In particular, one implementation of RPA through molecular sequestration has been proposed and implemented successfully in bacterial cells [34], [35], signifying important progress in principled design of biomolecular circuits.

On the other hand, our theoretical understanding of RPA in biomolecular systems is far from complete. From established tools of control theory, RPA as step disturbance rejection is thoroughly understood for linear dynamical systems, and the internal model principle could be used as a guideline for nonlinear systems [36]. However, biological constraints on implementable dynamics, such as variables need to be positive, make the design and implementation of RPA biomolecular circuits a challenging problem in general [33], [35]. Although significant progress has been made in RPA design by nonlinear analysis of biomolecular circuits, such approaches sensitively rely on the functional form of the production and degradation rates assumed in the model. More fundamentally, most biomolecular circuits are known to have desired properties like RPA only under certain parameter and state conditions, yet existing analysis and design methods often require RPA to hold globally. In comparison, RPA for linearized dynamics is local in nature, and it is described in a way that is independent of the rates' functional forms. Below, we show how RPA in linearized dynamics could be robustified by implementing it through structure.

RPA, i.e. step disturbance rejection, in a linear system corresponds to the transfer function evaluating to zero at zero frequency. This means $G(0) = d - \boldsymbol{c}\boldsymbol{A}^{-1}\boldsymbol{b} = 0$. Since $G(0)$ could be written as the determinant of a matrix, therefore the following definition and proposition.

Definition 9: A birth-death control system has *RPA* at reference point $(\boldsymbol{x}^*, w^*)$ if its linearized dynamics at this reference point in Eq (21) satisfies $z(t) \to 0$ as $t \to \infty$ for all constant disturbances $\delta \in \mathbb{R}$.

Proposition 10 ([18], [31], [33]): A birth death control system has RPA at reference point $(\boldsymbol{x}^*, w^*)$ if and only if

$$\det \begin{bmatrix} \boldsymbol{A} & \boldsymbol{b} \\ \boldsymbol{c} & d \end{bmatrix} = 0. \tag{26}$$

From Eq (22), we again see time-scales $\boldsymbol{\tau}$ and log derivatives are separated, prompting the following definition of structural RPA.

Definition 11: A birth-death control system has *structural RPA* at reference point $(\boldsymbol{x}^*, w^*)$ if it is RPA at this point for all non-negative analytic rate functions $\boldsymbol{f}^{\pm}$ and h that keep the log derivatives $(\boldsymbol{H}^A, \boldsymbol{H}^b, \boldsymbol{H}^c, H^d)$ invariant at $(\boldsymbol{x}^*, w^*)$.

Practically, the variations and uncertainties described in the above definition come down to the time scales $\boldsymbol{\tau}$ taking all positive values.

Theorem 12: A birth-death control system has structurral RPA at reference point $(\boldsymbol{x}^*, w^*)$ if and only if

$$\det \begin{bmatrix} \boldsymbol{H}^A & \boldsymbol{H}^b \\ \boldsymbol{H}^c & H^d \end{bmatrix} = 0. \tag{27}$$

Proof: It is necessary that the fold-change transfer function satisfies $\tilde{G}(0) = H^d - \boldsymbol{H}^c(\boldsymbol{H}^A)^{-1}\boldsymbol{H}^b = 0$, which is equivalent to Eq (27). Then since this condition is independent of $\boldsymbol{\tau}$ and only depends on the log derivative matrices, we see it is also sufficient for structural RPA. ■

V. Examples

Below we demonstrate the power of the log derivative approach to analyze stability and RPA properties of circuits and obtain further biological insights by considering two examples commonly found in biocontrol literature. Importantly, although Theorems 5 and 12 are simple applications of results from matrix analysis and linear control, the log derivative formalism is powerful in finding a direct and natural biological context to apply such results. Indeed, we show that many properties can often be determined at a glance, without calculations such as linearization. On the scalability side, although the examples selected here are simple for illustration purposes, the procedures used readily scales to large systems as the computations in Theorems 5 and 12 are scalable and the relationship between models and log derivatives are easily obtained as in Section II-C.

1) Incoherent feedforward circuit: Incoherent feedforward (IFF) circuits are both widely found in natural circuits [28], [30] and commonly used in synthetic circuit designs [29], [32], [33] to achieve RPA. We consider a simple IFF circuit below called the sniffer model [30]:

$$\begin{aligned} \dot{x}_1 &= w - \alpha x_1 x_2, \\ \dot{x}_2 &= \beta w - \gamma x_2 \end{aligned} \tag{28}$$

where x_2 catalyzes degradation of x_1, and w is a disturbance to the production rates of X_1 and X_2. Output is $y = x_1$, which states that we desire x_1's steady state concentration to be independent of disturbance w. We immediately write down the log derivative matrices using the basic calculation rules established in Section II-C:

$$\left[\begin{array}{c|c} \boldsymbol{H}^A & \boldsymbol{H}^b \\ \hline \boldsymbol{H}^c & H^d \end{array}\right] = \left[\begin{array}{cc|c} -1 & -1 & 1 \\ 0 & -1 & 1 \\ \hline 1 & 0 & 0 \end{array}\right], \tag{29}$$

where horizontal and vertical rules are added for clarity. We calculate the determinant to be zero, concluding that the circuit is structurally RPA. From Corollary 6, as $\boldsymbol{H}^A$ is triangular, we conclude that any positive fixed point of this circuit is structurally stable. Since this system is simple with constant log derivatives, this system has RPA and its positive fixed point is stable for all positive values of α, β, γ, w. Note that we could calculate fixed points ($x_1^* = \frac{\gamma}{\alpha\beta}$, $x_2^* = \frac{\beta w^*}{\gamma}$) and time scales ($\tau_1 = \frac{\gamma}{\alpha\beta w^*}$, $\tau_2 = \frac{1}{\gamma}$) and linearize the system, but structural properties are directly obtained without such calculations.

The structural stability of this system is not surprising, as triangular systems are known to have such properties from other methods. However, relating stability and RPA to log derivative matrices yields further biological insights.

For example, log derivative's robustness to changes in model's functional forms could be used to find alternative experimental implementations of the same structure. A variant of the IFF motif is the following circuit (adapted from [32] for plasmid copy number invariance):

$$\begin{aligned} \dot{x}_1 &= \frac{w}{x_2} - \alpha x_1, \\ \dot{x}_2 &= \beta w - \gamma x_2, \end{aligned} \tag{30}$$

where x_2 inhibits the production of x_1 instead of degrading it. This system also has structural RPA and stability as its log derivative matrices are the same as Eq (28).

As another example, the structural mindset can help us understand how properties like RPA are valid under one regime while invalid in other regimes. Consider a variant of Eq (30) where $f_1^+ = \frac{w}{k+x_2}$ instead, capturing saturation through a Hill function. Then $H_{12}^A = -\frac{x_2^*}{k+x_2^*}$ instead of -1. When $x_2^* \gg k$, $H_{12}^A \approx -1$, so Eq (29) hold asymptotically. Hence the regime with condition $x_2^* \gg k$ could be considered the structural RPA regime. For any variations in parameters and functional forms of the system, as long as the system is still inside this regime, the structural RPA property holds. For example, if we start with $H_{12}^A = -0.999$ in the structural RPA regime, then a 10-fold change in parameters (x_2^* and k) to drive the system away from this regime results in $H_{12}^A = -0.99$, still safely inside the structural RPA regime. This shows that structural regimes captured by log derivatives are powerfully robust to large parameter variations.

Above discussion suggests the view that a general birth-death system consists of several regimes, each with properties such as RPA implemented in its structure. This view is further explored in a biological context in [15], with discussions on multistability and oscillations.

2) Sequestration negative feedback circuit: [34] proposed a circuit design based on molecular sequestration that could serve as a control module achieving RPA for general classes of plants connected to it. This architecture and its tradeoffs are analyzed in [37]–[40]. We consider the following simple example with dilution from growth.

$$\begin{aligned}\dot{x}_1 &= w - (\eta x_1 x_2 + \gamma x_1),\\ \dot{x}_2 &= \theta x_3 - (\eta x_1 x_2 + \gamma x_2),\\ \dot{x}_3 &= \alpha \frac{x_1}{x_1 + k} - \gamma x_3,\end{aligned} \tag{31}$$

where x_1, x_2 together form the sequestration controller, and x_3 is the plant to be controlled. x_1 and x_2 sequester each other into a complex to be degraded. x_2 senses x_3's concentration as x_3 catalyzes the production of x_2, while x_1 actuates x_3 to track reference w by catalyzing the production of x_3. γ captures dilution from exponential growth.

Since the goal of this circuit is to make the concentration of x_3 asymptotically track w, the output is $y = \frac{x_3}{w}$. So the log derivatives are

$$\left[\begin{array}{c|c} \boldsymbol{H}^A & \boldsymbol{H}^b \\ \hline \boldsymbol{H}^c & H^d \end{array}\right] = \left[\begin{array}{ccc|c} -1 & -1+a_1 & 0 & 1 \\ -1+a_2 & -1 & 1 & 0 \\ 1-a_3 & 0 & -1 & 0 \\ \hline 0 & 0 & 1 & -1 \end{array}\right], \tag{32}$$

where $a_i \in (0,1)$ for $i = 1,2,3$. The particular values of a_i depend on the rates, e.g. $a_1 = \frac{\gamma_1 x_1^*}{\eta x_1^* x_2^* + \gamma_1 x_1^*}$. As argued in [34], making $a_1 = a_2 = 0$ achieves RPA. Indeed, the determinant of the above matrix is $a_2 - a_1(a_2 + a_3)$. When $a_1 = a_2 = 0$, this is zero and structural RPA is achieved.

Structural stability conditions on log derivatives could provide guidelines for circuit design and implementation. For example, although RPA is guaranteed when $a_1 = a_2 = 0$, which corresponds to no dilution of the controller molecules X_1 and X_2, $\boldsymbol{H}^A$ is not diagonally stable for any values of a_3. In contrast, if $a_1, a_2 > 0$, such as 0.01, then $\mathrm{Re}\boldsymbol{H}^A$ is negative definite for a wide range of a_3. This simple computation demonstrates that dilution of the controller molecules, albeit damaging to the disturbance rejection property of the controller, significantly improves stability of the closed loop system. This enhances the observations in [37], [38].

VI. Discussion

In this work, we argued that structural regimes of biomolecular circuits could be captured through log derivatives. We also demonstrated that fixed point stability and step disturbance rejection can be analyzed and designed through structure, independent of large variations in parameters and functional forms of circuit models.

This work builds on a train of thought that can be traced back to the very beginning of systems biology. Michaelis-Menten showed that time-scale separation and large concentration differences reveal distinct operating regimes of enzymatic regulations [8], [9]. In his pioneering work at the early days of systems biology [41], Savageau argued for the use of log dervatives as sensitivities of steady state concentrations to parameters, in order to study robustness. Furthermore, Savageau championed the view that a complex biomolecular circuit consists of several operating regimes. In particular, the concept of power systems is proposed that directly motivated the definition of birth-death systems and simple birth-death systems in this work. These pioneering ideas were later continued in gene regulation networks by Alon [29], and in stochasticity by Paulsson [24]. Works on these fronts became the foundational concepts and tools for systems biology.

This work, as well as several ongoing works, are attempts at formalizing many of the inspiring ideas from this train of thought, borrowing and creating tools from control theory, chemical reactions networks, and mathematics. This process reveals further implications and connections. Section II-B argues that log derivatives, rather than just steady state sensitivities, have their meaning rooted in the structures of biomolecular circuits, which can be formalized through time-scale separation with the application of implicit function theorem. This not only reveals the fascinating observation that log derivatives might form polytopes in general, but also provide a formal connection between powers, vertices of log derivative polytopes, and operating regimes of biomolecular circuits. Section III and IV relate log derivatives to stability and adaptation, and formally described the robustness to uncertainties in rates and functional forms in models that log derivatives could capture, extending the structural view for analysis and design of biomolecular circuits.

Another train of thought that this work borrowed much from is the theory of chemical reaction networks (CRNs) [16]. With strong mathematical rigor, many fascinating developments recently appeared from this community on robustness and stability based on graphical structures of CRNs [21], [42]–[44]. One challenge of CRN theory is to identify a class of biological CRNs to avoid pathologies from extreme-case CRNs [43]. Indeed, without biological restrictions, it has been shown that CRNs can perform Turing complete computations and produce arbitrary steady state distributions [45], [46]. This work suggests that a candidate for a biological subset of CRNs could be the set of binding and catalysis reactions. From the analysis in Section II-B, a time-scale separation argument connects the biological structures underlying systems biology models to the graphical structures of CRN theories, extending Michaelis-Menten approximations in an interpretable way.

Similar to the literature described above, the field of Metabolic Control Analysis (MCA) (see Chapter 13 of [47] for an introduction) uses log derivatives. In the context of metabolism, MCA considers log derivatives as elasticities and control coefficients that describe steady state sensitivities of metabolic fluxes to enzyme concentrations. In contrast, this work focuses on production-degradation structure of biomolecules in the context of synthetic biology, using log derivatives to capture dynamical regimes that biomolecular circuits could operate in. As a mathematical analogy, this work focuses on the vertices and shape of log derivative polytopes, rather than any particular point inside.

Lastly, there are many exciting questions left to be answered. One implication is that nonlinear biomolecular

systems may be more naturally viewed through the "basis" of simple birth-death systems instead of linear systems. This could be further developed using the framework of dissipative control [48] where each simple birth-death system defines a storage function that is valid in a region for the full system. Also, a foundational question is what classes of chemical reaction networks admit polytopic log derivatives. These questions are worth investigating, and we hope to answer them in another occasion in the near future.

REFERENCES

[1] M. Csete and J. C. Doyle, "Reverse engineering of biological complexity," *Science*, vol. 295, no. 5560, pp. 1664–1669, 2002.

[2] J. Doyle and M. Csete, "Motifs, control, and stability," *PLoS Biology*, vol. 3, no. 11, pp. 1872–1868, 2005.

[3] H. Kitano, "Towards a theory of biological robustness," *Molecular Systems Biology*, vol. 3, no. 1, p. 137, 2007.

[4] K. Zhou, J. C. Doyle, and K. Glover, *Robust and Optimal Control*. Pearson, 1995.

[5] B. Ø. Palsson, *Systems Biology: Constraint-based Reconstruction and Analysis*, stu - student edition ed. Cambridge University Press, 2015.

[6] F. A. Chandra, G. Buzi, and J. C. Doyle, "Glycolytic oscillations and limits on robust efficiency," *science*, vol. 333, no. 6039, pp. 187–192, 2011.

[7] R. Phillips and R. Milo, *Cell Biology by the Numbers*. New York: Garland Science, 2015.

[8] J. Gunawardena, "Time-scale separation – michaelis and menten's old idea, still bearing fruit," *The FEBS Journal*, vol. 281, no. 2, pp. 473–488, 2014.

[9] K. A. Johnson and R. S. Goody, "The original michaelis constant: Translation of the 1913 michaelis–menten paper," *Biochemistry*, vol. 50, no. 39, pp. 8264–8269, Oct 2011.

[10] J. Keener and J. Sneyd, *Mathematical Physiology I*. Springer-Verlag New York, 2009.

[11] D. Del Vecchio and R. M. Murray, *Biomolecular feedback systems*. Princeton University Press Princeton, NJ, 2015.

[12] J. Gunawardena, *Models in Systems Biology: The Parameter Problem and the Meanings of Robustness*. John Wiley Sons, Ltd, 2010, ch. 2, pp. 19–47.

[13] ——, "Models in biology: 'accurate descriptions of our pathetic thinking'," *BMC Biology*, vol. 12, no. 1, p. 29, Apr 2014.

[14] J. C. Doyle, "Even noisy responses can be perfect if integrated properly," *Cell Systems*, vol. 2, no. 2, pp. 73 – 75, 2016.

[15] J. P. Marken, F. Xiao, and R. M. Murray, "A geometric and structural approach to the analysis and design of biological circuit dynamics: a theory tailored for synthetic biology," *bioRxiv*, 2020.

[16] M. Feinberg, *Foundations of Chemical Reaction Network Theory*. Springer, 2020.

[17] E. O. Volt, H. A. Martens, and S. W. Omholt, "150 years of the mass action law," *PLOS Computational Biology*, vol. 11, no. 1, 2015.

[18] D. D. Vecchio and R. M. Murray, *Biomolecular Feedback Systems*, stu - student edition ed. Princeton University Press, 2015.

[19] K. R. Albe, M. H. Butler, and B. E. Wright, "Cellular concentrations of enzymes and their substrates," *Journal of Theoretical Biology*, vol. 143, no. 2, pp. 163 – 195, 1990.

[20] D. Del Vecchio, A. J. Ninfa, and E. D. Sontag, "Modular cell biology: retroactivity and insulation," *Molecular Systems Biology*, vol. 4, no. 1, p. 161, 2008.

[21] A. Dickenstein, M. P. Millán, A. Shiu, and X. Tang, "Multistationarity in structured reaction networks," *Bulletin of Mathematical Biology*, vol. 81, no. 5, pp. 1527–1581, May 2019.

[22] T. Bajbar and O. Stein, "Coercive polynomials: stability, order of growth, and newton polytopes," *Optimization*, vol. 68, no. 1, pp. 99–124, 2019.

[23] R. Murray, V. Chandrasekaran, and A. Wierman, "Newton polytopes and relative entropy optimization," 2020.

[24] J. Paulsson, "Models of stochastic gene expression," *Physics of Life Reviews*, vol. 2, pp. 157–175, 2005.

[25] F. Xiao, M. Fang, J. Yan, and J. C. Doyle, "Coupled reaction networks for noise suppression," *bioRxiv*, 2019. [Online]. Available: https://www.biorxiv.org/content/10.1101/440453v1

[26] O. Y. Kushel, "Unifying matrix stability concepts with a view to applications," *SIAM Review*, vol. 61, no. 4, pp. 643–729, 2019.

[27] A. M. Ostrowski, "Note on a theorem by hans schneider," *Journal of the London Mathematical Society*, vol. s1-37, no. 1, pp. 225–234, 1962.

[28] U. Alon, "Network motifs: theory and experimental approaches," *Nature Reviews Genetics*, vol. 8, no. 6, pp. 450–461, 2007.

[29] ——, *An Introduction to Systems Biology, Design Principles of Biological Circuits*. London: CRC, 2006.

[30] J. E. Ferrell, "Perfect and near-perfect adaptation in cell signaling," *Cell Systems*, vol. 2, no. 2, pp. 62–67, 2016.

[31] T.-M. Yi, Y. Huang, M. I. Simon, , and J. Doyle, "Robust perfect adaptation in bacterial chemotaxis through integral feedback control," *Proceedings of the National Academy of Sciences*, vol. 97, no. 9, 2000.

[32] T. H. Segall-Shapiro, E. D. Sontag, and C. A. Voigt, "Engineered promoters enable constant gene expression at any copy number in bacteria," *Nature Biotechnology*, vol. 36, no. 4, pp. 352–358, Apr 2018.

[33] F. Xiao and J. C. Doyle, "Robust perfect adaptation in biomolecular reaction networks," in *Proceedings of the 57th IEEE Conference on Decision and Control*, in-press.

[34] C. Briat, A. Gupta, and M. Khammash, "Antithetic integral feedback ensures robust perfect adaptation in noisy biomolecular networks," *Cell Systems*, vol. 2, no. 1, pp. 15 – 26, 2016.

[35] S. K. Aoki, G. Lillacci, A. Gupta, A. Baumschlager, D. Schweingruber, and M. Khammash, "A universal biomolecular integral feedback controller for robust perfect adaptation," *Nature*, vol. 570, no. 7762, pp. 533–537, Jun 2019.

[36] J. Huang, A. Isidori, L. Marconi, M. Mischiati, E. Sontag, and W. M. Wonham, "Internal models in control, biology and neuroscience," in *2018 IEEE Conference on Decision and Control (CDC)*, 2018, pp. 5370–5390.

[37] J. D. N Olsman, F Xiao, "Architectural principles for characterizing the performance of antithetic integral feedback networks," *Iscience*, vol. 14, pp. 277–291, 2019.

[38] N. Olsman, A. Baetica, F. Xiao, Y. P. Leong, R. Murray, and J. C. Doyle, "Hard limits and performance tradeoffs in a class of antithetic integral feedback networks," *Cell systems*, vol. 9, 2019.

[39] Y. Qian and D. Del Vecchio, "A singular singular perturbation problem arising from a class of biomolecular feedback controllers," *IEEE Control Systems Letters*, vol. 3, no. 2, pp. 236–241, 2019.

[40] Y. Qian and D. Del Vecchio, "Realizing ‘integral control’ in living cells: how to overcome leaky integration due to dilution?" *Journal of The Royal Society Interface*, vol. 15, no. 139, p. 20170902, 2018. [Online]. Available: https://royalsocietypublishing.org/doi/abs/10.1098/rsif.2017.0902

[41] M. Savageau, *Biochemical systems analysis. A study of function and design in molecular biology*. ADDISON WESLEY, 1976.

[42] F. Blanchini and E. Franco, "Structurally robust biological networks," *BMC Systems Biology*, vol. 5, no. 1, p. 74, May 2011.

[43] A. Sadeghimanesh and E. Feliu, "The multistationarity structure of networks with intermediates and a binomial core network," *Bulletin of Mathematical Biology*, vol. 81, no. 7, pp. 2428–2462, Jul 2019.

[44] M. Ali Al-Radhawi, D. Angeli, and E. D. Sontag, "A computational framework for a lyapunov-enabled analysis of biochemical reaction networks," *PLOS Computational Biology*, vol. 16, no. 2, pp. 1–37, 02 2020.

[45] L. Qian, D. Soloveichik, and E. Winfree, "Efficient turing-universal computation with dna polymers," in *DNA Computing and Molecular Programming*, Y. Sakakibara and Y. Mi, Eds. Berlin, Heidelberg: Springer Berlin Heidelberg, 2011, pp. 123–140.

[46] D. Cappelletti, A. Ortiz-Muñoz, D. F. Anderson, and E. Winfree, "Stochastic chemical reaction networks for robustly approximating arbitrary probability distributions," *Theoretical Computer Science*, vol. 801, pp. 64 – 95, 2020.

[47] A. Cornish-Bowden, *Fundamentals of Enzyme Kinetics*. Berlin: Wiley-Blackwell, 2012.

[48] M. Arcak, C. Meissen, and A. Packard, *Networks of Dissipative Systems*. Springer, 2011.